International Conference on Mathematics, Computational Methods & Reactor Physics (M&C 2009)
Saratoga Springs, New York, May 3-7, 2009, on CD-ROM, American Nuclear Society, LaGrange Park, IL (2009)

SEMI-CONSISTENT DIFFUSION SYNTHETIC ACCELERATION FOR DISCONTINUOUS DISCRETIZATIONS OF TRANSPORT PROBLEMS

Anthony P. Barbu and Marvin L. Adams
Department of Nuclear Engineering
Texase A&M University
College Station, TX, 77843-3133
apbarbu@gmail.com; mladams@tamu.edu

ABSTRACT

We have developed a diffusion synthetic acceleration (DSA) method for discontinuous finite element methods (DFEMs) in which the diffusion operator is constructed from the matrices that appear in the transport discretization. This allows the diffusion operation to be coded once (in terms of single-cell transport matrices) and then used by any DFEM or related method that is implemented in the code. The diffusion operation first solves a global system for a continuous function and then performs local (cell by cell) calculations to obtain the desired discontinuous function. We cast the DSA scheme as a preconditioner to set the stage for use with Krylov methods. Using Fourier analysis we determine the spectral radius of the iteration operator for a one-group infinite-homogeneous medium transport problem. The results of simple test problems agree with the Fourier analysis results. The method behaves similarly to other partially consistent methods: a peak in spectral radius is obtained for square cells on the order of one mean free path (mfp), and this peak increases in value and broadens in range as the cell aspect ratio increases. The peak spectral radius stays bounded well below unity except for large aspect ratios. Based on these results and results from previous researchers, we conclude that the method's preconditioner should work quite well within Krylov solvers. Further, its definition in terms of single-cell transport methods offers an attractive implementation advantage (a single block of coding to handle all DFEM and related methods).

Key Words: Transport, Preconditioner, Acceleration, DSA, DFEM

1. INTRODUCTION

The deterministic transport solution of practical problems requires iterative techniques to solve the large systems of equations that arise from discretization. A simple iteration procedure, "source iteration," often converges slowly when used for thick problems with scattering ratios near unity [1]. The current state of the art is to use a Krylov method with a diffusion preconditioner, which is equivalent to putting a Krylov solver "around" a diffusion-synthetic acceleration (DSA) method [7]. However, the diffusion preconditioner must be tailored to the transport discretization – "consistent" with it in some sense – to ensure effectiveness [4][6][7]. Guided by work done by Wareing for the BiLinear Discontinuous (BLD) discretization in two dimensions [5], we have developed a preconditioner for general discontinuous finite-element method (DFEM) discretizations in one, two, and three dimensions. We describe this preconditioner here, apply it to a Piecewise-Linear-Discontinuous (PWLD) transport discretization [3], analyze the convergence properties of the resulting iteration operator through Fourier analysis and test problems, and compare the results to results from a related Inconsistent DSA method.

Our preconditioner uses a global continuous finite-element diffusion solution and then performs local single-cell operations to generate a discontinuous finite-element solution from the continuous solution. This is the basic procedure introduced by Wareing [5] for the BLD scheme. The result is a discontinuous correction obtained at approximately the cost of a continuous finite-element diffusion solution. Our main enhancements to Wareing's approach are a generalization to arbitrary discontinuous finite-element methods, and development of a procedure whereby the diffusion matrices are built from the matrices used by the transport DFEM scheme. This enables us to write a preconditioning scheme that needs minor additions at most when new transport discretizations are introduced.

We show that while our method is much simpler to implement and requires much less computational effort than a fully consistent diffusion scheme, it retains many of the attractive properties of the fully-consistent Diffusion Synthetic Acceleration (DSA) method.

2. ITERATION EQUATIONS

We begin by introducing our notation for finite element matrices. Then we define the transport and correction equations and their variables. Once defined, we use these equations to detail the derivation of the proposed method. Finally, we cast the iteration scheme in operator notation to determine the form of the accelerator as a preconditioner, and to facilitate the Fourier analysis of the proposed method.

2.1. Operator Definition

For brevity, our equations are discretized only spatially, leaving angular discretization to be made independently of spatial. First we define matrices that appear in the discretized equations. Superscripts denote the order of the derivative of weight and basis functions respectively; subscripts denote the domain of integration (τ for a volume integral over current cell, and $\partial\tau_k$ for surface integral over face k of cell τ); an arrow above a matrix means that it contains spatial vectors (e.g. has $\{x, y, z\}$ components); underscores denote mathematical vectors (lists of unknowns) due to discretization.

$$
\begin{aligned}
&\underline{\underline{A}}_{\tau}^{00} = \int_{\tau} d^3 r \underline{b}\left(\vec{r}\right)\underline{b}^T\left(\vec{r}\right), && \underline{\underline{A}}_{\tau}^{11} = \int_{\tau} d^3 r \vec{\nabla}\underline{b}\left(\vec{r}\right)\cdot\vec{\nabla}\underline{b}^T\left(\vec{r}\right)\\
&\underline{\underline{A}}_{\partial\tau_k}^{00} = \int_{\partial\tau_k} d^2 r \underline{b}\left(\vec{r}\right)\underline{b}^T\left(\vec{r}\right), && \vec{\underline{\underline{A}}}_{\partial\tau}^{00} = \sum_{k=1}^{K}\vec{n}_k\,\underline{\underline{A}}_{\partial\tau_k}^{00}\\
&\vec{\underline{\underline{A}}}_{\tau}^{10} = \left(\vec{\underline{\underline{A}}}_{\tau}^{01}\right)^T = \int_{\tau} d^3 r \vec{\nabla}\underline{b}\left(\vec{r}\right)\underline{b}^T\left(\vec{r}\right), && \vec{\underline{\underline{A}}}_{\partial\tau_k}^{01} = \int_{\partial\tau_k} d^2 r \underline{b}\left(\vec{r}\right)\vec{\nabla}\underline{b}^T\left(\vec{r}\right)
\end{aligned}
\tag{1}
$$

Here $\vec{n}_k$ is the outward unit normal of face k of cell τ, and K is the number of faces of a cell. These matrices are cell-dependent quantities that can be identified for arbitrary DFEM (and

related) discretizations. All but two of these ($\underline{\underline{A}}_{\tau}^{11}$ and $\underline{\underline{\bar{A}}}_{\partial\tau_k}^{01}$) are used in the transport DFEM solution. The DFEM transport equation, in this matrix notation, for one cell is:

$$\begin{aligned}\sum_{\bar{n}_k\cdot\bar{\Omega}<0} \bar{\Omega}\bullet\bar{n}_k \underline{\underline{A}}_{\partial\tau_k}^{00} \underline{\psi}_{\langle k\rangle}^{(l+1/2)}\left(\bar{\Omega}\right) + \sum_{\bar{n}_k\cdot\bar{\Omega}>0} \bar{\Omega}\bullet\bar{n}_k \underline{\underline{A}}_{\partial\tau_k}^{00} \underline{\psi}^{(l+1/2)}\left(\bar{\Omega}\right) - \bar{\Omega}\bullet\underline{\underline{A}}_{\tau}^{10} \underline{\psi}^{(l+1/2)}\left(\bar{\Omega}\right) \\ +\sigma_t \underline{\underline{A}}_{\tau}^{00} \underline{\psi}^{(l+1/2)}\left(\bar{\Omega}\right) = \frac{\sigma_s}{4\pi} \underline{\underline{A}}_{\tau}^{00} \underline{\phi}^{(l)} + \underline{\underline{A}}_{\tau}^{00} \underline{Q}\end{aligned} \tag{2}$$

$$\underline{\phi}^{(l+1/2)} = \int_{4\pi} d\Omega' \underline{\psi}^{(l+1/2)}\left(\bar{\Omega}'\right) \tag{3}$$

Here $\underline{\psi}$ is the vector of angular dependent variables, $\underline{\phi}$ is the vector of angle-integrated—scalar—variables, $\bar{\Omega}$ is the unit vector in the direction of particle flow, $\underline{Q}$ contains all sources that do not depend on $\underline{\phi}$, σ_t is the total interaction cross section, and σ_s is the scattering cross section. Superscripts denote iteration step. The subscript $\langle k\rangle$ denotes quantities just outside of the cell sharing face k (upstream quantities). Superscripts in parenthesis, (l) and (l+1/2), are iteration indices. Simple source iteration would set $\phi^{(l+1)} = \phi^{(l+1/2)}$. DSA sets $\phi^{(l+1)} = \phi^{(l+1/2)} + F$, where F is an additive correction obtained by solving a diffusion problem.

Our DSA procedure begins with the creation of an inconsistent continuous diffusion correction. For this we employ continuous versions of the discontinuous basis functions used for the transport discretization. If the transport problem has specified-incident boundary conditions, the continuous correction satisfies a diffusion equation with vacuum boundary conditions:

$$\sum_{\substack{\text{cells } \tau \\ \text{at vertex } i}} \left[\underline{E}_{\tau,i}\right]^T \left\{ \sum_{\substack{k=1 \\ \partial\tau_k\in\Gamma}}^{N} \frac{1}{2} \underline{\underline{\bar{A}}}_{\partial\tau_k}^{00} + \frac{1}{3\sigma_t} \underline{\underline{A}}_{\tau}^{11} + \sigma_{a,\tau} \underline{\underline{A}}_{\tau}^{00} \right\} \underline{\underline{H}}_{\tau} \underline{F}_C = \sum_{\substack{\text{cells } \tau \\ \text{at vertex } i}} \left[\underline{E}_{\tau,i}\right]^T \sigma_{s,\tau} \underline{\underline{A}}_{\tau}^{00} \left[\underline{\phi}^{(l+1/2)} - \underline{\phi}^{(l)}\right]_{\tau} \tag{4}$$

Here $\underline{F}_C$ represents the continuous scalar corrections (typically one number per vertex in the grid), $\underline{\underline{H}}_{\tau}$ maps the appropriate elements of $\underline{F}_C$ to a local vector for cell τ, $\left[\underline{E}_{\tau,i}\right]^T$ selects the row of cell τ's matrices that corresponds to vertex i, σ_a is the absorption cross section, and Γ is the boundary of the problem domain. This equation is solved globally to obtain the continuous correction.

It is straightforward to manipulate Eq. (2), along with its counterpart for the converged solution, into a similar equation for the exact correction that would produce the converged solution if added to the (l+1/2) iterate [2]. The 0th and 1st moments of this discrete correction equation for one cell are:

$$\sum_{k=1}^{N} \underline{\underline{A}}_{\partial\tau_k}^{00} \bar{n}_k \bullet \underline{\bar{G}}_{D,k} - \underline{\underline{\bar{A}}}_{\tau}^{10} \bullet \underline{\bar{G}}_D + \sigma_a \underline{\underline{A}}_{\tau}^{00} \underline{F}_D = \sigma_s \underline{\underline{A}}_{\tau}^{00} \left[\underline{\phi}^{(l+1/2)} - \underline{\phi}^{(l)}\right] \tag{5}$$

$$\sum_{k=1}^{N} \vec{n}_k \underline{\underline{A}}^{00}_{\partial\tau_k} \frac{1}{3} \underline{F}_{D,k} - \underline{\underline{\vec{A}}}^{10}_{\tau} \frac{1}{3} \underline{F}_D + \sigma_t \underline{\underline{A}}^{00}_{\tau} \underline{\vec{G}}_D = 0 . \tag{6}$$

Here $\underline{F}_D$ is the zero-angular-moment (scalar) correction, $\underline{\vec{G}}_D$ is a correction to the first-angular-moment (current), and subscripts D denote discontinuous variables. The surface corrections (with subscript D,k) contain hidden complexity, for they depend on scalar and current corrections on both sides of the surface. This couples all of the scalar and current unknowns in the problem and makes the fully consistent equations costly to solve.

2.2. Proposed Method

One form of inconsistent DSA would use the continuous system of equations given by Eq. (4) to obtain a correction for each vertex, which would then be added to the scalar unknowns of all cells that meet at the given vertex. Consistent DSA would use a more expensive global discontinuous solution of Eqs. (5)-(6) to obtain a correction for each unknown. The proposed method uses both sets of equations, utilizing the continuous correction to simplify the global discontinuous equations. We use the following procedure to localize the discontinuous correction equation for each cell so that it does not use information from neighboring cells:

1) We substitute discontinuous surface scalar corrections, $\underline{F}_{D,k}$, in Eq. (6) with the continuous correction obtained in the global solution, $\underline{F}_C$ (a good approximation of the fully consistent surface correction if there is only a small jump in scalar corrections between cells):

$$\underline{F}_{D,k} \rightarrow \underline{\underline{H}}_{\tau} \underline{F}_C . \tag{7}$$

2) We solve the resulting equation for the discontinuous current correction, $\underline{\vec{G}}_D$:

$$\underline{\vec{G}}_D = -\underline{\underline{D}}_{\tau} \left[\underline{\underline{\vec{A}}}^{00}_{\partial\tau} \underline{\underline{H}}_{\tau} \underline{F}_C + \underline{\underline{\vec{A}}}^{10}_{\tau} \underline{F}_D \right], \qquad \text{where } \underline{\underline{D}}_{\tau} \equiv \frac{1}{3\sigma_t} \left[\underline{\underline{A}}^{00}_{\tau} \right]^{-1} \tag{8}$$

3) We replace the discontinuous surface current correction, $\underline{\vec{G}}_{D,k}$, in Eq. (5) with a continuous correction, $\underline{\vec{G}}_C$:

$$\underline{\vec{G}}_{D,k} \rightarrow \underline{\vec{G}}_C \tag{9}$$

4) We define $\underline{\vec{G}}_C$ in terms of $\underline{F}_C$, $\underline{F}_D$ and $\underline{\vec{G}}_D$ by forcing the continuous corrections to give the same outgoing partial currents as the discontinuous corrections:

$$\sum_{k=1}^{N} \underline{\underline{A}}_{\partial\tau_k}^{00} \int_{\vec{n}_k\cdot\vec{\Omega}>0} d\Omega \vec{n}_k \cdot\vec{\Omega}\left[\underline{\underline{H}}_{\tau}\underline{F}_C + 3\vec{\Omega}\cdot\underline{\vec{G}}_C\right] = \sum_{k=1}^{N} \underline{\underline{A}}_{\partial\tau_k}^{00} \int_{\vec{n}_k\cdot\vec{\Omega}>0} d\Omega \vec{n}_k \cdot\vec{\Omega}\left[\underline{F}_D + 3\vec{\Omega}\cdot\underline{\vec{G}}_D\right], \tag{10}$$

which yields:

$$\sum_{k=1}^{N} \underline{\underline{A}}_{\partial\tau_k}^{00} \vec{n}_k \cdot\underline{\vec{G}}_C = \sum_{k=1}^{N} \underline{\underline{A}}_{\partial\tau_k}^{00} \left[\frac{\alpha_{k,1}}{3\alpha_2}\left(\underline{F}_D - \underline{\underline{H}}_{\tau}\underline{F}_C\right) + \vec{n}_k \cdot\underline{\vec{G}}_D\right] \tag{11}$$

where:

$$\alpha_{k,1} \equiv \frac{1}{4\pi}\int_{\vec{n}_k\cdot\vec{\Omega}>0} d\Omega \vec{n}_k\cdot\vec{\Omega} \quad \text{and} \quad \alpha_{k,2} \equiv \frac{1}{4\pi}\int_{\vec{n}_k\cdot\vec{\Omega}>0} d\Omega\, \vec{n}_k\cdot\vec{\Omega}\,\vec{n}_k\cdot\vec{\Omega} \tag{12}$$

We use the equality in Eq. (10) to substitute again into the substitution made in Eq. (8). To summarize all of the manipulations made to Eq. (5):

$$\sum_{k=1}^{N} \underline{\underline{A}}_{\partial\tau_k}^{00} \left[\frac{\alpha_{k,1}}{3\alpha_2}\left(\underline{F}_D - \underline{\underline{H}}_{\tau}\underline{F}_C\right) + \vec{n}_k \cdot\underline{\vec{G}}_D\right] - \underline{\underline{\vec{A}}}_{\tau}^{10}\cdot\underline{\vec{G}}_D + \sigma_a \underline{\underline{A}}_{\tau}^{00}\underline{F}_D = \sigma_s \underline{\underline{A}}_{\tau}^{00}\left[\underline{\phi}^{(l+1/2)} - \underline{\phi}^{(l)}\right], \tag{13}$$

5) We use the divergence theorem to simplify terms involving $\underline{\vec{G}}_D$:

$$\sum_{k=1}^{N} \underline{\underline{A}}_{\partial\tau_k}^{00}\left[\vec{n}_k\cdot\underline{\vec{G}}_D\right] - \underline{\underline{\vec{A}}}_{\tau}^{10}\cdot\underline{\vec{G}}_D = \underline{\underline{\vec{A}}}_{\tau}^{01}\cdot\underline{\vec{G}}_D, \tag{14}$$

Resulting in:

$$\sum_{k=1}^{N} \underline{\underline{A}}_{\partial\tau_k}^{00} \frac{\alpha_{k,1}}{3\alpha_2}\left(\underline{F}_D - \underline{\underline{H}}_{\tau}\underline{F}_C\right) + \underline{\underline{\vec{A}}}_{\tau}^{01}\cdot\underline{\vec{G}}_D + \sigma_a \underline{\underline{A}}_{\tau}^{00}\underline{F}_D = \sigma_s \underline{\underline{A}}_{\tau}^{00}\left[\underline{\phi}^{(l+1/2)} - \underline{\phi}^{(l)}\right], \tag{15}$$

We can now see the effect of the substitutions. The equation is similar to the original equation, plus a surface term containing the difference between continuous and discontinuous scalar corrections.

6) We substitute for $\underline{\vec{G}}_D$ using the equation from step (2):

$$\begin{aligned}\sum_{k=1}^{N} \underline{\underline{A}}_{\partial\tau_k}^{00} \frac{\alpha_{k,1}}{3\alpha_2}\left(\underline{F}_D - \underline{\underline{H}}_{\tau}\underline{F}_C\right) - \underline{\underline{\vec{A}}}_{\tau}^{01}\cdot\underline{\underline{D}}_{\tau}\left[\underline{\underline{\vec{A}}}_{\partial\tau}^{00}\underline{\underline{H}}_{\tau}\underline{F}_C + \underline{\underline{\vec{A}}}_{\tau}^{10}\underline{F}_D\right] \\ + \sigma_a \underline{\underline{A}}_{\tau}^{00}\underline{F}_D = \sigma_s \underline{\underline{A}}_{\tau}^{00}\left[\underline{\phi}^{(l+1/2)} - \underline{\phi}^{(l)}\right]\end{aligned} \tag{16}$$

7) We solve for the desired discontinuous scalar correction:

$$\underline{F}_D = \left(\sum_{k=1}^{N} \frac{\alpha_{k,1}}{3\alpha_2} \underline{\underline{A}}^{00}_{\partial\tau_k} + \underline{\underline{\vec{A}}}^{01}_{\tau} \bullet \underline{\underline{D}}_{\tau} \underline{\underline{\vec{A}}}^{10}_{\tau} + \sigma_a \underline{\underline{A}}^{00}_{\tau} \right)^{-1} \left[\begin{array}{c} \left(\sum_{k=1}^{N} \frac{\alpha_{k,1}}{3\alpha_2} \underline{\underline{A}}^{00}_{\partial\tau_k} + \underline{\underline{\vec{A}}}^{01}_{\tau} \bullet \underline{\underline{D}}_{\tau} \underline{\underline{\vec{A}}}^{00}_{\partial\tau} \right) \underline{\underline{H}}_{\tau} \underline{F}_C \\ + \sigma_s \underline{\underline{A}}^{00}_{\tau} \left(\underline{\phi}^{(l+1/2)} - \underline{\phi}^{(l)} \right) \end{array} \right] \tag{17}$$

This is our "semi-consistent" discontinuous correction for cell τ. We apply this correction as follows:

$$\underline{\phi}^{(l+1)} = \underline{\phi}^{(l+1/2)} + \underline{F}_D \tag{18}$$

While Eq. (17) looks cumbersome, it requires inversion of only a one-cell matrix. This matrix does not change between successive iterations, and may be stored to prevent repeated calculation.

2.3. Operator Notation

We show that we can express source iteration as "Richardson" iteration and a DSA scheme as *preconditioned* Richardson iteration. Once cast as a preconditioned iteration, it is simple to convert to a Krylov iteration with the same preconditioner. In operator notation, the transport sweep and scalar-flux update may be written as:

$$L\psi^{(l+1/2)} = S\phi^{(l)} + q \tag{19}$$

$$\phi^{(l+1/2)} = W\psi^{(l+1/2)} \tag{20}$$

Where:

$$L = \left[\sum_{\vec{n}_k \cdot \vec{\Omega} < 0} \vec{n}_k \bullet \vec{\Omega} \underline{\underline{A}}^{00}_{\partial\tau_k} \right]_{\langle k \rangle} + \sum_{\vec{n}_k \cdot \vec{\Omega} > 0} \vec{n}_k \bullet \vec{\Omega} \underline{\underline{A}}^{00}_{\partial\tau_k} - \vec{\Omega} \bullet \underline{\underline{\vec{A}}}^{10}_{\tau} + \sigma_t \underline{\underline{A}}^{00}_{\tau} \tag{21}$$

$$S = \frac{\sigma_s}{4\pi} \underline{\underline{A}}^{00}_{\tau} \tag{22}$$

$$q = \underline{\underline{A}}^{00}_{\tau} \underline{Q} \tag{23}$$

$$W = \int_{4\pi} d\Omega \approx \sum_{m=1}^{M} w_m \tag{24}$$

For the operator W we use discrete ordinates, where w_m are quadrature weights and M is the number of quadrature points. Solving for $\phi^{(l+1/2)}$:

$$\phi^{(l+1/2)} = WL^{-1}S\phi^{(l)} + WL^{-1}q = \left(I - A\right)\phi^{(l)} + b \tag{25}$$

We write the continuous diffusion correction equation as:

$$L_C F_C = S_C \left(\phi^{(l+1/2)} - \phi^{(l)} \right) \tag{26}$$

where,

$$L_C = \sum_{\substack{\text{cells } \tau \\ \text{at vertex } i}} \left[\underline{E}_{\tau,i} \right]^T \left\{ \sum_{\substack{k=1 \\ \partial\tau_k \in \Gamma}}^{N} \frac{1}{2} \overline{\underline{\underline{A}}}^{00}_{\partial\tau_k} + \frac{1}{3\sigma_t} \underline{\underline{A}}^{11}_{\tau} + \sigma_{a,\tau} \underline{\underline{A}}^{00}_{\tau} \right\} \underline{\underline{H}}_{\tau} \tag{27}$$

$$S_C = \sum_{\substack{\text{cells } \tau \\ \text{at vertex } i}} \left[\underline{E}_{\tau,i} \right]^T \sigma_{s,\tau} \underline{\underline{A}}^{00}_{\tau} \tag{28}$$

We write the discontinuous diffusion correction equation as:

$$L_D F_D = S_D \left(\phi^{(l+1/2)} - \phi^{(l)} \right) + R F_C \tag{29}$$

where,

$$L_D = \sum_{k=1}^{N} \frac{\alpha_{k,1}}{3\alpha_2} \underline{\underline{A}}^{00}_{\partial\tau_k} + \overline{\underline{\underline{A}}}^{01}_{\tau} \bullet \underline{\underline{D}}_{\tau} \overline{\underline{\underline{A}}}^{10}_{\tau} + \sigma_a \underline{\underline{A}}^{00}_{\tau} \tag{30}$$

$$S_D = \sigma_s \underline{\underline{A}}^{00}_{\tau} \tag{31}$$

$$R = \left(\sum_{k=1}^{N} \frac{\alpha_{k,1}}{3\alpha_2} \underline{\underline{A}}^{00}_{\partial\tau_k} + \overline{\underline{\underline{A}}}^{01}_{\tau} \bullet \underline{\underline{D}}_{\tau} \overline{\underline{\underline{A}}}^{00}_{\partial\tau} \right) \underline{\underline{H}}_{\tau} \tag{32}$$

The update equation remains:

$$\phi^{(l+1)} = \phi^{(l+1/2)} + F_D \tag{33}$$

Solving for $\phi^{(l+1)}$ in terms of only $\phi^{(l)}$ we obtain:

$$\phi^{(l+1)} = \left[I - PA \right] \phi^{(l)} + Pb, \tag{34}$$

which is a preconditioned Richardson iteration with preconditioner P given by:

$$P \equiv I + L_D^{-1} \left\{ S_D + R L_C^{-1} S_C \right\}. \tag{35}$$

3. RESULTS

Our results fall into two categories: Fourier analysis and test problem results. Our Fourier analysis finds the spectral radius of the iteration operator for simple infinite-medium model problems. For our numerical test problems we estimate the iterative spectral radius, which is the error-reduction factor per iteration after many iterations. In both cases, we use S_4 quadrature.

The spectral radius is found for various values of horizontal mfp, $\sigma_t \Delta x$, and vertical mfp, $\sigma_t \Delta y$, and also for different aspect ratios, the ratio of the vertical mfp to the horizontal mfp which equals $\Delta y / \Delta x$.

3.1. Fourier Analysis

To obtain the spectral radius of method under certain conditions, we choose a problem of infinite medium, uniform rectangular mesh, with constant material properties. We make the standard Fourier ansatz:

$$\underline{\phi}^{(l)} = \omega^l \underline{\phi}^* e^{i\sigma_t \vec{\lambda} \cdot \vec{r}} \tag{36}$$

We recognize that each mode is independent of the others, and can be evaluated within one cell with a certain kind of periodic boundary condition, since each cell may be viewed as a translation of its neighbors in an infinite homogeneous system. Substituting this ansatz creates an eigenvalue problem for ω, taking the form of finding the eigenvalues of a 4x4 matrix (in our 2D problems) for each value of $\vec{\lambda}$. The eigenvalues are evaluated numerically using Matlab.

The spectral radius is the maximum eigenvalue of the operator over $\{\lambda_x \sigma_t \Delta x, \lambda_y \sigma_t \Delta y\} \in \circ^2$. The search space is reduced by recognizing the modes have period of 2π, and is symmetric about π, reducing the domain of $\{\lambda_x \sigma_t \Delta x, \lambda_y \sigma_t \Delta y\} \in (0,\pi) \times (0,\pi)$.

Figure 1 shows spectral radius of the Fourier analysis operator for various horizontal mfp and cells defined by an aspect ratio of one and one hundred. Figure 2 is a contour plot of spectral radius over a range of horizontal mfp from .001 to 1000 and aspect ratios of 1 to 1000. These results are for the Piecewise Linear Discontinuous (PWLD) finite element method. Results for the BLD method are similar.

Our results are similar to those observed by Wareing et al. [5]. This is as expected, for our method is a generalization of theirs. In particular, the Fourier analysis predicts excellent performance for square cells but degraded performance for thick cells with high aspect ratios, limiting to a spectral radius of *c* for very thick cells with very high aspect ratios. Previous work has shown that using the operator of Wareing et al. as a preconditioner within a Krylov method removes the slow-convergence issue for cells with high aspect ratio [6], for the BLD spatial discretization with 2D rectangular cells. We anticipate that the same will hold for our

generalized version of this operator for various DFEMs on various cell shapes in 2D and 3D; this is the motivation for our work.

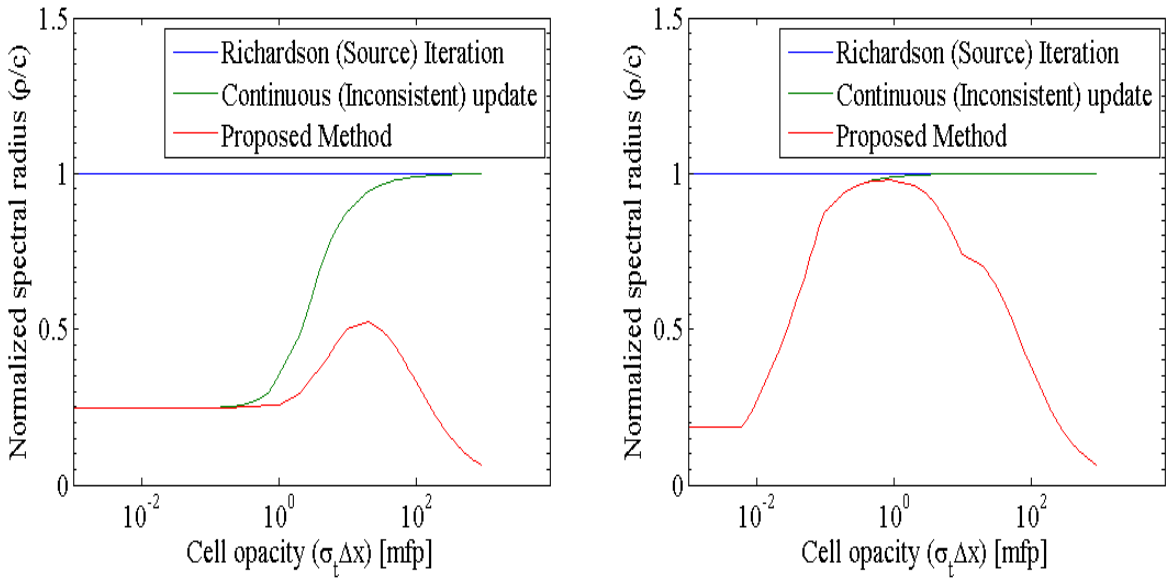

Figure 1. Normalized spectral radii from Fourier analysis with *c* of .95 for aspect ratios 1 (left plot) and 100 (right plot).

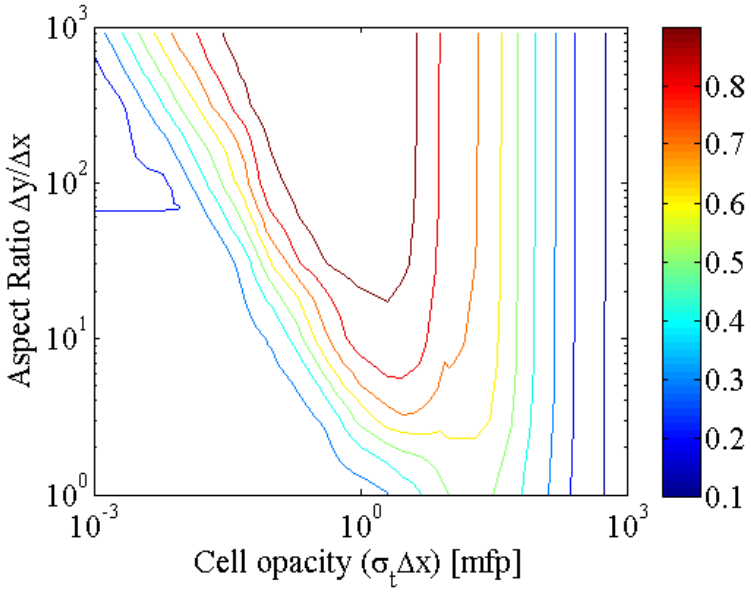

Figure 2. Normalized spectral radii from Fourier analysis with *c* of .95 varying aspect ratio and cell opacity.

3.2. Test Problem

To mimic the Fourier analysis as closely as possible, we choose a homogeneous medium, isotropic scattering problem with the same scattering ratio and material properties. In particular, we choose a vacuum boundary and zero source such that the correct solution is exactly zero. Choosing a non-zero initial guess makes a non-zero error which should reduce in magnitude by the spectral radius after many iterations. Thus, the error is the norm of the current solution, and after many iterations the spectral radius is the ratio of the current iteration error to the previous iteration error.

We attempt to make the problem optically thick so that neutron leakage is a small quantity. However, to make the entire problem optically thick and have optically thin cells would require a prohibitive amount of cells. Thus, leakage becomes a dominant factor of loss for the thin-cell test problems, and the spectral radius of the operator is reduced dramatically.

Figure 3 shows spectral radius of the test-problem operator for various mfp and cells defined by an aspect ratio of one and one hundred. Figure 4 is a contour plot of spectral radius over a range of mfp from .001 to 1000 and aspect ratios of 1 to 1000. These results are from the PWLD method.

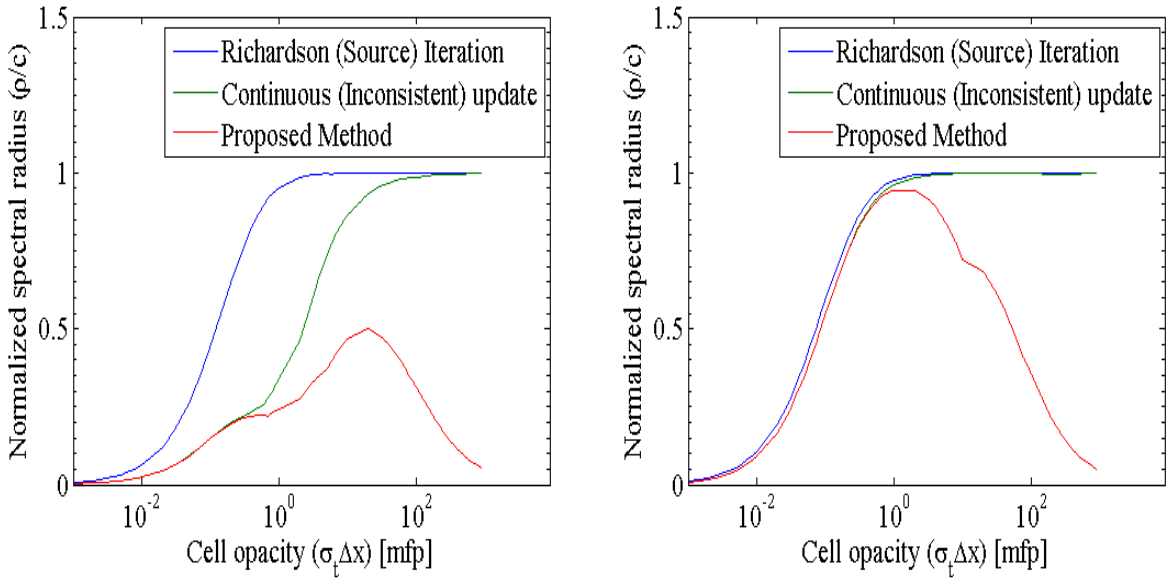

Figure 3. Normalized spectral radii from test problem with *c* of .95 for cells of aspect ratio 1, and 100.

We see that except for the thin-cell problems with significant leakage, the results from numerical test problems agree very closely with the results from the Fourier analysis. This gives us confidence that the analysis is correct.

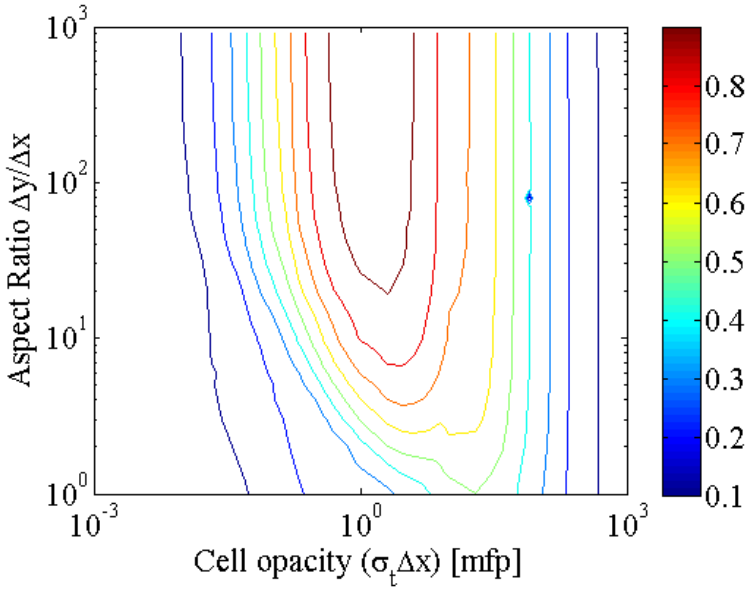

Figure 4. Normalized spectral radii from test problem with *c* of .95 varying aspect ratio and cell opacity.

We also study the effects of the scattering ratio value on the test problem spectral radius. Figure 5 shows the spectral radius of a problem similar to the square cells (aspect ratio of 1) problem in Figure 3, but with scattering ratios of .99 and .999 respectively.

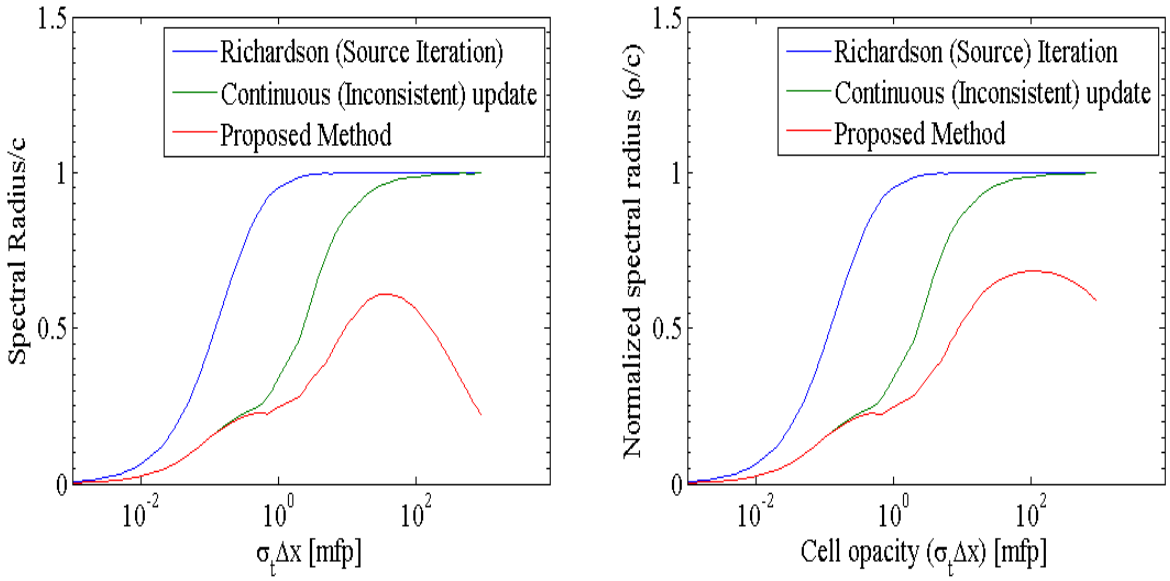

Figure 5. Normalized spectral radii from test problem with *c* of .99 and .999 for cells of aspect ratio 1.

The peak of our operator increases in value and shifts to higher cell thicknesses as the scattering ratio approaches unity.

4. CONCLUSIONS

We have modified a consistent discontinuous DSA equation by replacing surface quantities with an expression in terms of continuous DSA corrections. The result applies the continuous DSA correction as a boundary condition for each cell, which then permits the construction of semi-consistent discontinuous corrections independently in each cell.

When leakage is not a dominant loss mechanism, numerical test results agree with our infinite-medium (no-leakage) Fourier analyses. The results show this method is efficient for either thick or thin problems with square cells, while the convergence performance degrades as cell aspect ratio increases. Previous work with a similar iterative operator has shown that using the operator as a preconditioner in a Krylov iteration produces excellent performance even for cells with high aspect ratios. We expect the same to hold for our generalized version of this operator. Thus, we expect that the method presented here provides a path to rapid iterative convergence for a variety of DFEMs on a variety of kinds of spatial grids. We expect to test this on radiative-transfer problems in 2D and 3D in the near future.

The method described here has several attractive features. First, its global diffusion solution has only one unknown per vertex, and it uses a symmetric positive-definite operator. It obtains its discontinuous additive corrections via independent single-cell solutions that use the continuous solution as boundary conditions for each cell. These features cause the preconditioner to be relatively inexpensive. Second, our preconditioner is defined by manipulating the single-cell matrices that arise from the underlying transport DFEM. This offers the possibility of writing general coding for the preconditioner in terms of these matrices, such that the coding does not need to be changed when a new DFEM is added to the code. This can save a great deal of time and effort.

ACKNOWLEDGMENTS

We thank Todd Wareing for laying the foundation for this research. We thank Jim Morel for many helpful conversations.

REFERENCES

1. M.L. Adams, “Discontinuous Finite Element Transport Solutions in Thick Diffusive Problems,” *Nuclear Science and Engineering*, **137**, 298-333 (2001).
2. M.L. Adams, E.W. Larsen, “Fast Iterative Methods for Discrete-Ordinates Particle Transport Calculations,” *Progress in Nuclear Energy*, **40**, No. 1, 3-159 (2002)..
3. T. Bailey, “A Piecewise Linear Finite Element Discretization of the Diffusion Equation,” Master Thesis, TAMU (2006).

4. E.W. Larsen, "Unconditionally Stable Diffusion Synthetic Acceleration Methods for the Slab Geometry Discrete Ordinates Equations Part 1: Theory," *Nuclear Science and Engineering*. **82**, 47 (1982).
5. T.A. Wareing, "Asymptotic Diffusion Accelerated Discontinuous Finite Element Methods for Transport Problems," *Los Alamos National Laboratory Report*, LA-12425-T(1992).
6. J.S. Warsa, T.A. Wareing, and J.E. Morel, "Krylov Iterative Methods and the Degraded Effectiveness of Diffusion Synthetic Acceleration for Multidimensional Sn Calculations in Problems with Material Discontinuities," *Nuclear Science and Engineering*, **147**, 218-248 (2004).
7. J.S.Warsa, T.A.Wareing, and J.E. Morel, "Fully-Consistent Diffusion Synthetic Acceleration of Linear Discontinuous Sn Transport Discretizations on Unstructured Tetrahedral Meshes," *Nuclear Science and Engineering*, **141**, 235-251 (2002).